CoA Memo M and P No. 50

September, 1964

THE COLLEGE OF AERONAUTICS

DEPARTMENT OF PRODUCTION AND INDUSTRIAL ADMINISTRATION

A new approach to the mechanics of metal cutting

- by -

P.L.B. Oxley

Introduction

A number of equations have been derived for predicting the shear angle (ϕ in Fig. 1) in orthogonal metal cutting. The best known of these is due to Merchant (1) who by assuming that the value of shear angle would be such as to give a minimum expenditure of work obtained the relation

$$\phi = \frac{\pi}{4} + \frac{\alpha}{2} - \frac{\lambda}{2} \qquad (1)$$

where α is the tool rake angle (Fig. 1) and λ is the mean angle of friction between the chip and the tool along the tool-chip interface.

Lee and Shaffer (2) applied ideal slip-line field theory to the problem and obtained the equation

$$\phi = \frac{\pi}{4} + \alpha - \lambda \qquad (2)$$

Equations (1) and (2) predict that an increase in rake angle or a decrease in friction angle will give an increase in shear angle and this is consistent with experience. However, both equations also predict a unique value of ϕ for a given value of $\lambda - \alpha$ and it can be seen from the experimental values of ϕ given in figure 2 that this is not the case. It is clear from experiments that ϕ varies with material and cutting speed, and yet except for associated variations in λ equations (1) and (2) take no account of these.

By allowing that the shear strength along the shear plane (AB in Fig. 1) would increase with increase in the normal stress on this plane Merchant (1) derived the equation

$$2\phi = C + \alpha - \lambda \qquad (3)$$

where C measures the dependance of shear strength on normal stress. Subsequent work has shown that the values of C required to satisfy experimental work cannot be explained in terms of the dependance of shear strength on normal stress. It is also difficult to understand from this equation why ϕ should vary with cutting speed and feed in the way it is known to.

More recently Kobayashi and Thomsen (3) have introduced the concept of effectiveness which is essentially a measure of the departure from the minimum energy solution of Merchant (1), i.e. equation (1). An effectiveness of unity corresponds to equation (1) and smaller values of effectiveness give a lower value of ϕ for a given value of $\lambda - \alpha$ than equation (1). By choosing suitable values of effectiveness it is possible to satisfy any experimental value of ϕ. Although useful in collating experimental

data, e.g. it appears that effectiveness is constant for a given material and cutting speed, the value of the analysis is limited by the lack of any obvious fundamental relationship between effectiveness and work material properties or cutting speed.

Variable flow stress theory

It is implicit in all of the above theories that the normal stress acting on the shear plane does not vary along the length of the shear plane. That this is only true for a material whose flow stress does not change during cutting can be shown as follows.
Let us assume for simplicity that the removed metal chip is formed in a parallel sided shear zone as shown in fig. 3, with AB, CD and EF directions of maximum shear stress (and incidentally directions of maximum shear strain rate as well). Consider the equilibrium of the small element of the shear zone shown in fig. 4.

As the work material passes through this zone its flow stress will change as a result of work-hardening, thermal softening etc. Therefore, let the shear flow stress along CD (i.e. the initial shear flow stress at zero plastic strain) be $k - \frac{\Delta k}{2}$, and let the shear flow stress along EF be $k + \frac{\Delta k}{2}$. The total change in shear flow stress is then Δk. Resolving forces parallel to AB gives

$$(p + \Delta p)\Delta s_1 + (k - \frac{\Delta k}{2})\Delta s_2 = p\Delta s_1 + (k + \frac{\Delta k}{2})\Delta s_2$$

and simplifying

$$\Delta p = \frac{\Delta k}{\Delta s_1} \Delta s_2 \qquad (4)$$

where Δp is the change in hydrostatic stress across the element, Δs_1 is the width of the shear zone and Δs_2 is measured along AB. Because AB is a direction of maximum shear stress the hydrostatic stress p (Fig. 4) is also the normal stress on AB, equation (4) therefore expresses the variation of this stress along AB. It is clear from this equation that the normal stress p is only constant along AB when $\Delta k = 0$, i.e. for a material of constant flow stress.

The flow stress of a material is known to vary in cutting and it is common experience that the chip is much harder than the parent material from which it is removed. Any theory which neglects this effect can therefore be expected to give poor results. Let us now consider a theory based on equation (4).

If we neglect any forces on the clearance face of the tool, AB will transmit the resultant cutting force. The shear force on AB is

$$F_s = k \frac{t}{\sin \phi} \qquad (5)$$

where t (Fig. 3) is the depth of cut and therefore $\frac{t}{\sin \phi}$ is the length of AB, and k is the shear flow stress along AB. The normal compressive force on AB can be calculated from the normal stress distribution along AB. For a parallel sided shear zone $\frac{\Delta k}{\Delta s_1}$ in equation (4) will be constant and the normal stress distribution along AB will be linear. Therefore, the total normal compressive force acting on AB will be

$$F_N = \frac{p_A + p_B}{2} \frac{t}{\sin \phi} \tag{6}$$

where p_A and p_B are the hydrostatic (i.e. normal) stresses at A and B respectively. The angle of inclination of the resultant cutting force with AB (θ in Fig. 3) can now be found from equations (5) and (6), that is

$$\tan \theta = \frac{F_N}{F_s} = \frac{p_A + p_B}{2k} \tag{7}$$

The angle θ can also be expressed in terms of the frictional condition along the tool-chip interface and as can be seen from Fig. 5

$$\theta = \phi + \lambda - \alpha \tag{8}$$

In comparing shear angle equations and experimental results it is usual to plot values of ϕ against values of $\lambda - \alpha$. θ in equation (8) is then the intercept on the ϕ axis (i.e. the value of ϕ for $\lambda - \alpha = o$). In the Lee and Shaffer solution (equation (2)) $p_A = p_B = k$ and $\theta = 45°$. In the present solution θ can be calculated from equation (7) once p_A and p_B are known. p_A (which is compressive) is found from the free surface condition just ahead of A (Fig. 3), that is

$$p_A = k\{1 + 2(\tfrac{\pi}{4} - \phi)\} \tag{9}$$

and by applying equation (4) between A and B

$$p_B = p_A - \frac{\Delta k}{\Delta s_1} \frac{t}{\sin \phi} \tag{10}$$

For a material whose flow stress increases during cutting, therefore, p_B will have a lower compressive (even tensile) value than p_A.

It is known from experiments that the length to width ratio of the shear zone (i.e. $\frac{t}{\Delta s_1 \sin \phi}$) is reasonably constant for a range of work materials and cutting conditions. Therefore, it is the variations in Δk which have the greatest influence on the values of p_B and hence θ. The larger the increase in shear flow stress during cutting the smaller the

value of p_B and therefore from equation (7) the smaller the value of θ. In other words materials which work-harden rapidly tend, by reason of equation (10), to produce a lower normal force on AB, and hence lower values of θ than materials with low work-hardening rates.

In terms of shear angle results small values of θ (i.e. small values of intercept on the ϕ against $\lambda - \alpha$ graph) give small values of shear angle ϕ. Therefore, materials which work-harden rapidly can be expected, according to the present theory, to machine with smaller shear angles than materials with low work-hardening rates. With this in mind let us now reconsider the experimental values of shear angle given in Fig. 2.

The effective stress-effective strain curves for the work materials represented in Fig. 2 are given in Fig. 6. These were obtained from compression tests by Kobayashi and Thomsen (4) who also did the cutting tests for the experimental values of shear angle given in Fig. 2. In cutting the strain-rates are high (up to 10^6 per sec) and the stress-strain curves in Fig. 6, which were obtained at very low strain-rates, do not really apply. However, it seems reasonable to assume that a material which work-hardens rapidly at low strain-rates will work-harden relatively rapidly at high strain-rates. Following this line of reasoning we can propose that materials with high rates of work-hardening as measured by a 'static' test (e.g. Fig. 6) will machine with smaller values of shear angle than materials with low rates of work-hardening.

A detailed analysis by Oxley and Welsh (5) has shown that the work-hardening parameter of importance in estimating shear angles is $\frac{m}{k}$, where m is the average slope of the stress-strain curve above an effective strain of 0.2 and k ($k = \frac{\sigma_{eff}}{\sqrt{3}}$) is taken at an effective strain of 0.5.

Values of $\frac{m}{k}$ obtained in this way for the materials shown in Fig. 6 are given in table 1. From this table we would expect the range of values of ϕ to be lowest for alpha brass and then in the order SAE 1112 Annealed, SAE 1112 as received, 6061-T6 Al, and 2024-T4 Al. The experimental values of ϕ for these materials (Fig. 2) confirm this trend.

	MATERIAL	m/k
1	SAE 1112 steel (as received)	.14
2	2024-T4 aluminium alloy	.10
3	SAE 1112 steel (annealed)	.25
4	6061-T6 aluminium alloy	.11
5	Alpha brass	.42

TABLE 1

Figure 7 shows stress-strain curves for four conditions of SAE 4135 steel and table 2 gives the corresponding values of $\frac{m}{k}$. Experimental

	MATERIAL	m/k
1	SAE 4135 (Rc - 35)	.06
2	SAE 4135 (Rc - 26)	.09
3	SAE 4135 (as received)	.21
4	SAE 4135 (annealed)	.21

TABLE 2

values of Φ (Figs. 8 and 9) for the four conditions of the material again show that the higher the value of $\frac{m}{k}$ the lower is the range of values of Φ.

The present theory also throws light on the variation of shear angle with cutting speed. It is well known that at low cutting speeds the shear angle tends to be much smaller than at high cutting speeds. It is also known from research in the materials field that an increase in strain-rate (which would follow from an increase in cutting speed) gives a decrease in m and an increase in k, i.e. $\frac{m}{k}$ decreases. Therefore, at high cutting speeds we have a high strain-rate a low values of $\frac{m}{k}$ and therefore, according to the theory, a high value of shear angle. In reference (5) calculations were made to show the influence of cutting speed on shear angle. These are reproduced in Fig. 10 and it can be seen that the agreement between theory and experiment is good.

Finally we can say something about the tendency of some materials to machine with a discontinuous chip. If the hydrostatic stress in the region of B (Fig. 3) has a low compressive value or becomes tensile then the chip is likely to crack in this region. From our theory (equation (10)) we know that high rates of work-hardening give small compressive or even tensile values of p_B. Therefore, we might expect that materials which work-harden rapidly will tend to machine with discontinuous chips. This is known in practice to be the case.

References

1. M.E. Merchant — J. Appl. Phys. 16, 267 and 318 (1945)
2. F.H. Lee and B.W. Shaffer — J. Appl. Mech. 18, 405 (1951)
3. S. Kobayashi and E.G. Thomsen — Trans. A.S.M.E. paper 61-Prod-2 (1961)
4. S. Kobayashi and E.G. Thomsen — Trans. A.S.M.E. 81, 251 (1959)
5. P.L.B. Oxley and M.J.M. Welsh — Proc. 4th Int. M.T.D.R. Conf. Manchester (1963)
6. S. Kobayashi, R.P. Herzog S.M. Eggleston and E.G. Thomsen — Trans. A.S.M.E. 82, 333 (1960)
7. D. Kececioglu — Trans. A.S.M.E. 80, 158 (1958)
8. M.C. Shaw, M.H. Cook and I. Finnie — Trans. A.S.M.E. 75, 273 (1953)
9. P.L.B. Oxley — Leeds University, Ph.D., Thesis (1957)

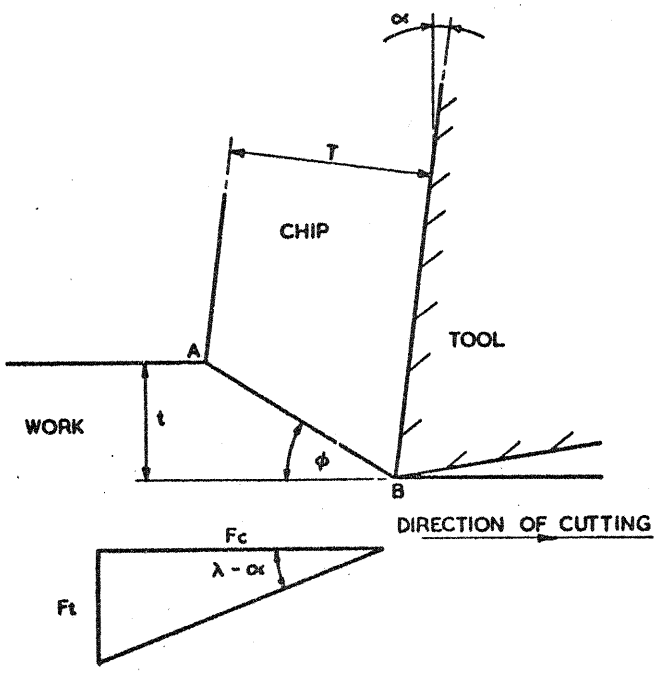

FIG. 1 SHEAR PLANE MODEL OF CHIP FORMATION

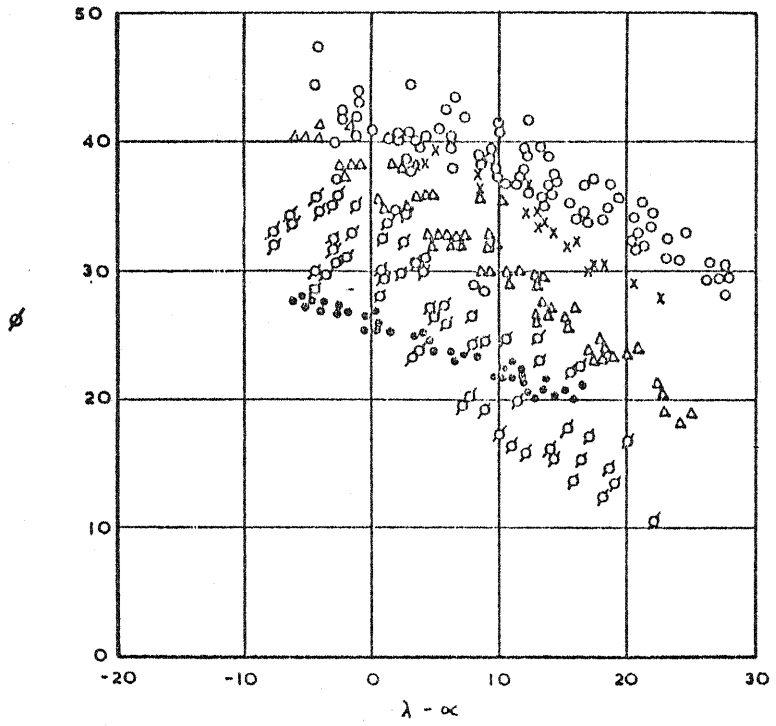

FIG. 2 Shear angle values for materials shown in Fig. 6 (Kobayashi and Thomsen).

2024-T4 aluminium alloy	○
6061-T6 aluminium alloy	×
SAE 1112 steel (as received)	△
SAE 1112 steel (annealed)	⌀
Alpha brass	●

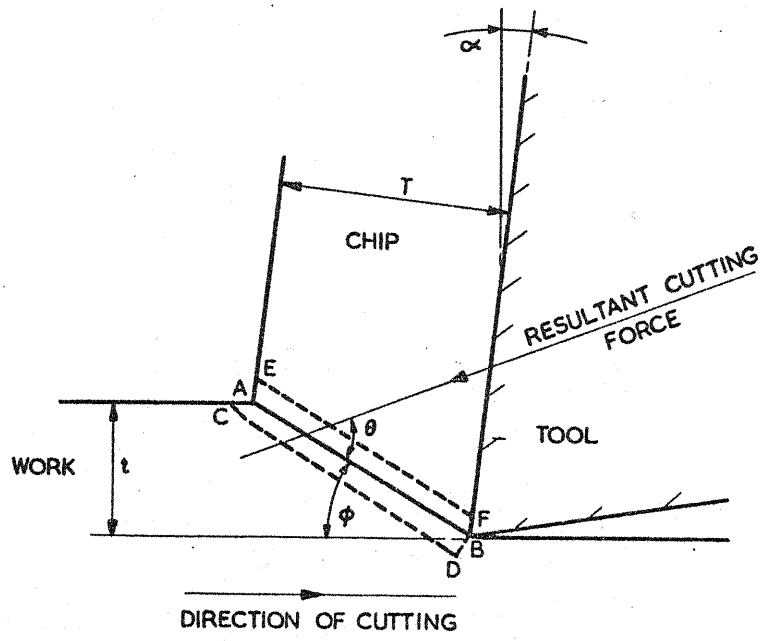

FIG. 3. SHEAR ZONE MODEL OF CHIP FORMATION

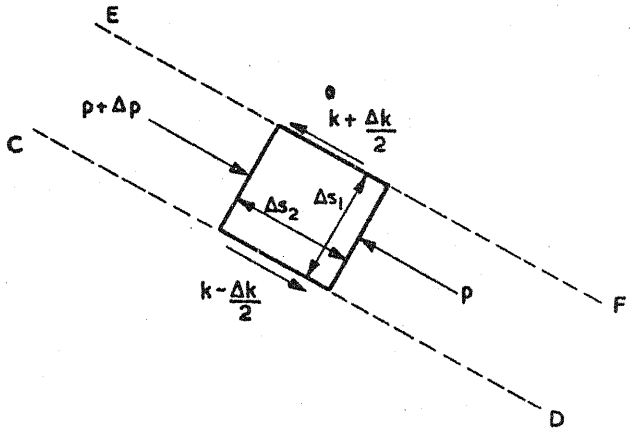

FIG. 4. SHEAR ZONE ELEMENT

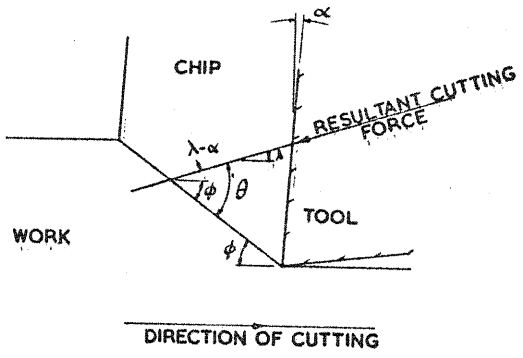

FIG.5. DIAGRAM SHOWING RELATIONSHIP
$\theta = \phi + \lambda - \alpha$

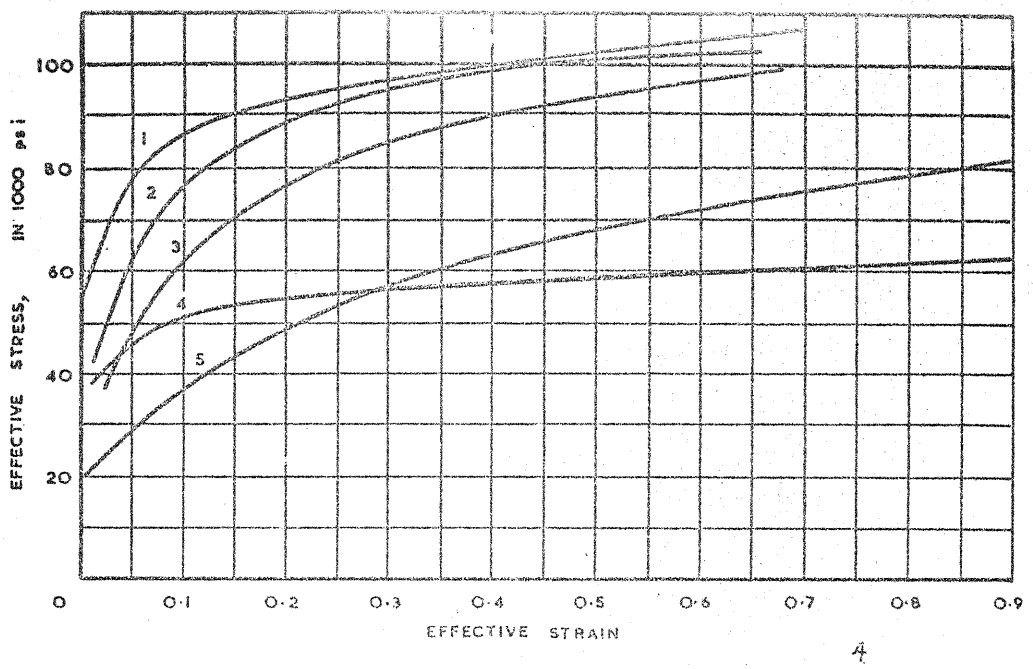

4

FIG. 6. Effective stress–strain curves (Kobayashi and Thomsen).

1. SAE 1112 steel (as received)
2. 2024-T4 aluminium alloy
3. SAE 1112 steel (annealed)
4. 6061-T6 aluminium alloy
5. Alpha brass

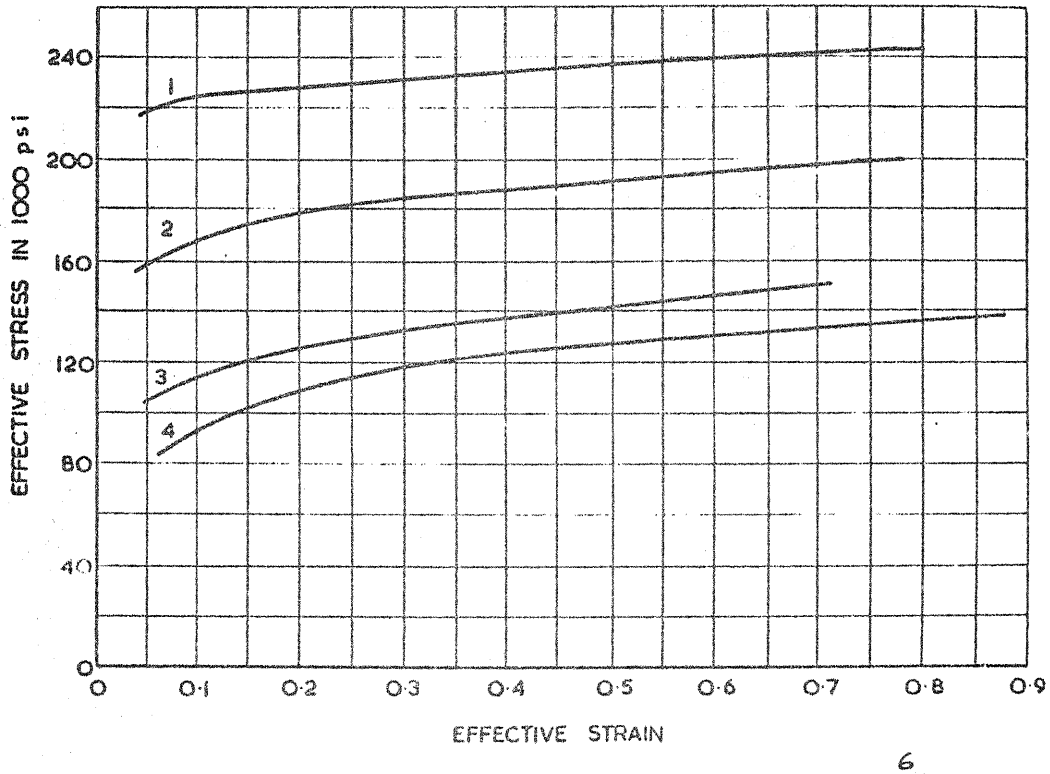

6

FIG. 7. EFFECTIVE STRESS-STRAIN CURVES (KOBAYASHI ET AL)

1. SAE 4135 RC-35
2. SAE 4135 RC-28
3. SAE 4135 AS REC.
4. SAE 4135 Annealed

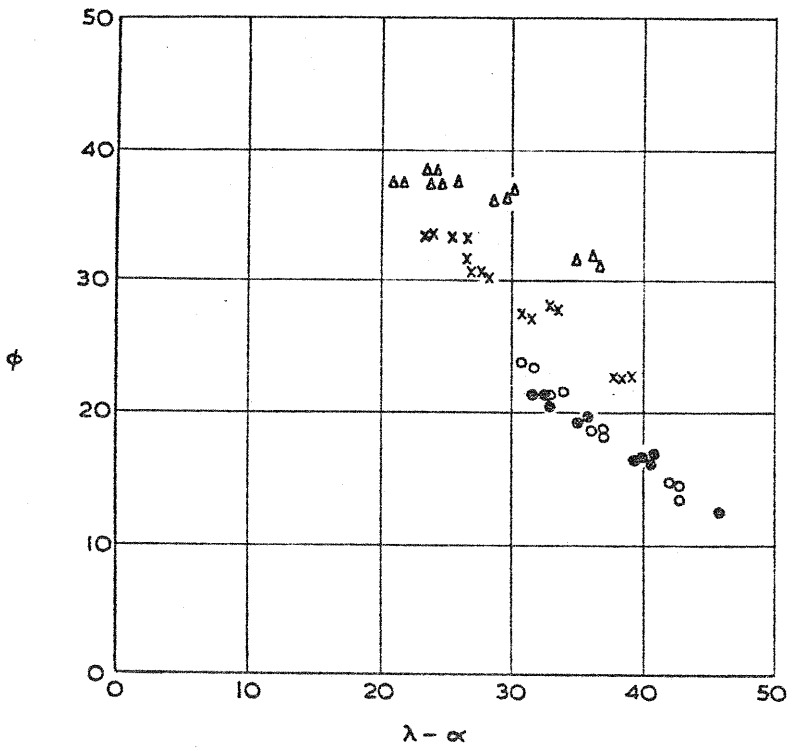

FIG. 8 SHEAR ANGLE VALUES FOR MATERIALS SHOWN IN FIG 7

$\alpha = 0^\circ$ U = 334 f.p.m.

SAE 4135 RC-35 Δ
SAE 4135 RC-26 x
SAE 4135 AS-REC o
SAE 4135 Annealed ●

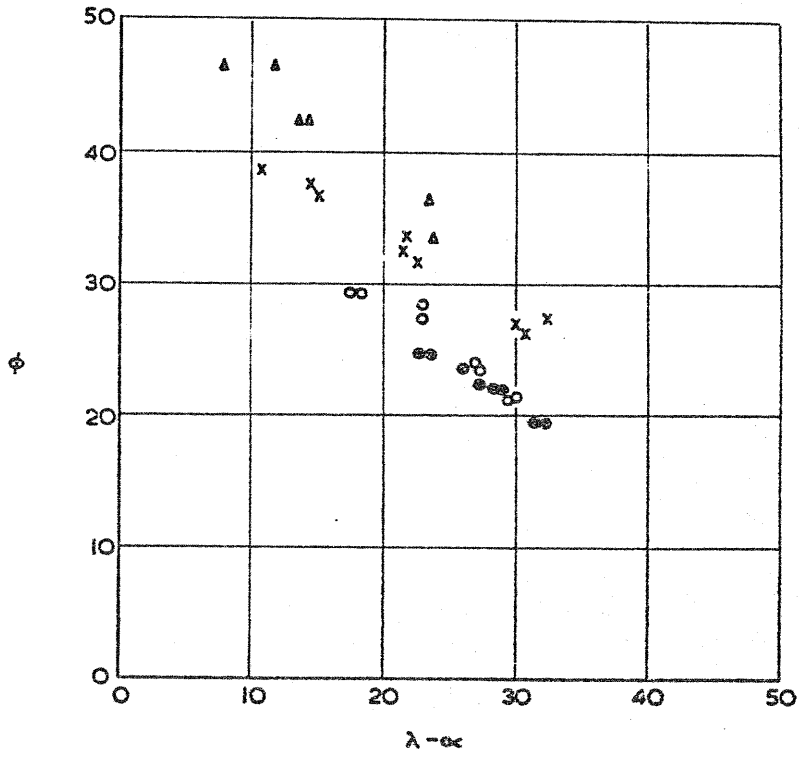

FIG. 9 SHEAR ANGLE VALUES FOR MATERIALS SHOWN IN FIG. 7

$\alpha = 20^\circ$ U = 393 f.p.m.

SAE 4135 RC-35 Δ
SAE 4135 RC-26 x
SAE 4135 AS-REC o
SAE 4135 Annealed ●